Contrast Sensitivity Functions for HDR Displays

Minjung Kim[1], Maliha Ashraf[2], María Pérez-Ortiz[1,3], Jasna Martinovic[4], Sophie Wuerger[2] and Rafał K. Mantiuk[1];
[1]Department of Computer Science and Technology, University of Cambridge; [2]Cognitive & Clinical Neuroscience Group, University of Liverpool; [3]Department of Computer Science, University College London; [4]School of Psychology, University of Aberdeen

Abstract

Contrast sensitivity functions (CSFs) characterize the sensitivity of the human visual system at different spatial frequencies. However, little is known about CSFs at luminances above 1000 cd/m^2, especially for color. Here, we measured contrast sensitivities at background luminances from 0.02 cd/m^2 to 7000 cd/m^2 and for three color directions (black-white or achromatic, red-green, and yellow-violet). Stimuli were Gabor patches of various spatial frequencies (0.125 to 6 cpd), displayed on a custom-built high dynamic range display (peak luminance: 15,000 cd/m^2). We found that achromatic contrast sensitivity has an inverted U-shape as a function of background luminance, with peak sensitivity at 200 cd/m^2, while red-green and yellow-violet contrast sensitivities were monotonic functions of background luminance, saturating at 200 cd/m^2. Based on these measurements, we developed a model that predicts contrast sensitivity for the average observer. This model is intended for applications in high dynamic range imaging.

Introduction

Spatial vision refers to the ability to see variations of image intensity across space; it is one of the basic elements in our understanding of human vision. Existing work has largely focused on stimulus visibility as a function of spatial frequency [4, 18, 7, 14, 16, 13, 3]. A typical experiment measures the minimum contrast required to detect a target stimulus (contrast threshold), which indicates the sensitivity of the visual system to that spatial frequency (contrast sensitivity); the value of contrast sensitivity as a function of spatial frequency is known as the *contrast sensitivity function* (CSF). See [20] for a model and comprehensive review of achromatic contrast detection.

However, little is known about contrast sensitivity at very high and very low luminance levels. For achromatic contrast, measurements exist for luminance up to approximately 1000 cd/m^2 [19, 12]; no measurements exist for color contrast at such extreme levels.

Here, we describe contrast sensitivity over a wide range of frequencies, colors, and luminances. We also present a computational model of contrast sensitivity for an average (standard) observer. As such, our data and model together inform how the visual system operates at the very high and low luminance levels that high dynamic range (HDR) displays can reach. See [23] for a more detailed description of our work, including additional experiments.

Contrast Detection Experiment

We measured contrast thresholds for target stimuli with in three color directions and at luminances ranging from 0.02 cd/m^2 (low mesopic) to 7000 cd/m^2 (high photopic).

Stimuli

The stimuli were Gabor patches created by multiplying a Gaussian envelope with a sinusoidal grating centered at the peak of the Gaussian (Fig. 1). The gratings were of spatial frequencies $f = 0.5$, 1, 2, 4, or 6 cycles per degree of visual angle (cpd), and the width of the Gaussian envelope was $\sigma = 0.5\,f^{-1}$ visual degrees; thus, all stimuli showed the same number of cycles ('fixed-cycles'), but varied in size as a function of f. Such stimuli allowed us to treat the visible number of cycles, and therefore stimulus size, as an additional parameter for modeling.

The Gabors were modulated around a neutral grey (white) that was metameric with D65 (CIE 1931 x, y = 0.3127, 0.3290). Color modulations were defined in Derrington-Krauskopf-Lennie (DKL) space [6], whose cardinal directions correspond to combinations of cone responses: achromatic ($L+M$), red-green ($L-M$), and yellow-violet ($S-(L+M)$). DKL space allows a device-independent definition of the chromatic stimulus modulations, and thus, comparisons with CSF measurements in literature.

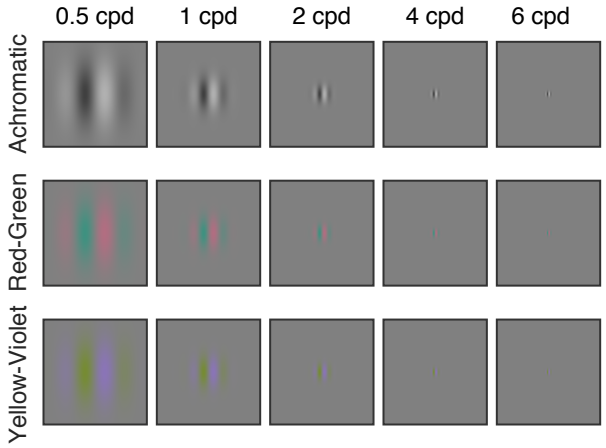

Figure 1: Fixed-cycles stimuli. Width of the Gaussian envelope was half of the wavelength, $\sigma = 0.5f^{-1}$ (deg).

Apparatus

Stimuli were displayed on two custom-built HDR displays, identical except for peak luminance (Liverpool: 4,000 cd/m^2; Cambridge: 15,000 cd/m^2). Each display consisted of an LCD panel (9.7", 2048×1536 px iPad 3/4 retina display; product code: LG LP097QX1) and a DLP projector (Optoma X600 in Cambridge, Acer P1276 in Liverpool; both 1024×768 px). We replaced the backlight of the LCD with the DLP [17]; see Fig. 2. We removed the color wheel of the DLP, tripling its maximum brightness, and introduced a Fresnel lens (focal length: 32 cm) behind the LCD to direct light towards the observer. The maximum contrast of the display was 1,000,000:1.

The display was calibrated and driven by custom software and Psychtoolbox [9]. For geometric calibration, we found homographic and mesh-based transformations that best mapped between DLP and LCD pixel coordinates. We used software compensation to handle spatial non-uniformity.

For color calibration, we converted the spectral emissions of the display (Fig. 2) to L-, M-, and S-cone responses [5]. For

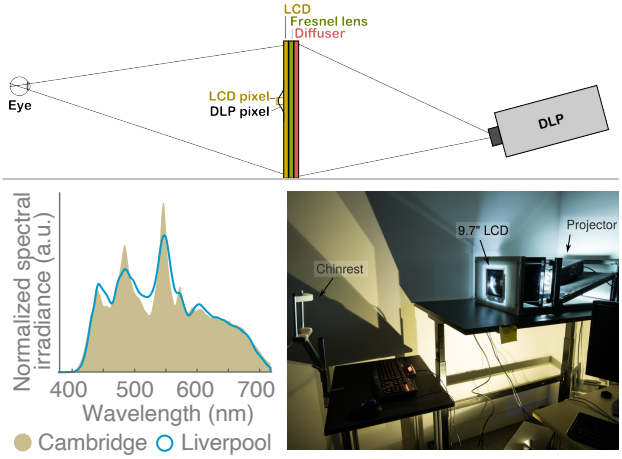

Figure 2: Top. Schematic diagram of the general HDR display design. Lower left. Emission spectra of the displays. Lower right. Photograph of the HDR display.

the LCD, we fitted the responses to a gain-offset-gamma display model [2]; for the DLP, we used a 1-dimensional look-up table.

Using spatio-temporal dithering on the LCD and bit-stealing on the DLP extended the bit-depth of the display to 10 bits per color channel. The target image was factorized into DLP and LCD components such that their product formed the desired image [17]. The display driver was written in the OpenGL shading language (GLSL) to factorize and render images in real-time.

Observers

Twenty-one color-normal observers with normal or corrected-to-normal visual acuity participated in the experiment (mean age = 30.0). All provided informed consent, in accordance with respective University Ethics Committees.

Procedure

The experiment was grouped into sessions by mean luminance, $l = 0.02, 0.2, 2, 20, 200, 2000, 7000\,\mathrm{cd/m^2}$. For sessions at 0.02 and 0.2 $\mathrm{cd/m^2}$, observers adapted to a darkened room for 5 to 10 minutes prior to starting, and remained in the room until the end of the session. Within a session, spatial frequencies and color directions were interleaved in a random order.

Observers were seated 91 cm from the HDR display, which subtended $12.5° \times 9.4°$. Head position was stabilized with a chin rest, but observers were allowed to move their eyes in order to examine stimuli. All viewing was binocular.

Measurements were made using a 4-alternative-forced-choice procedure, in which observers indicated the quadrant of the display that contained a Gabor patch. The stimulus was positioned at 3.77° eccentricity, and the contrast was determined using a QUEST procedure [21]. The stimulus was displayed until response; between trials, a noise mask was presented for 500 ms.

Results

Figure 3 shows the results. At luminances of 2 $\mathrm{cd/m^2}$ and higher, the contrast sensitivities showed a classic band-pass response, with peak response at 1 to 2 cpd. The gradual change from a low-pass shape at 0.02 $\mathrm{cd/m^2}$ and 0.2 $\mathrm{cd/m^2}$ to the typical band-pass shape above 0.2 $\mathrm{cd/m^2}$ is similar to the results of [19]. It is likely that measuring frequencies below 0.5 cpd would have revealed a band-pass shape at all luminances.

Figure 4 recasts the data as a function of background luminance. For achromatic stimuli, contrast sensitivity followed an inverted U-shape, with the lowest sensitivity at 0.02 $\mathrm{cd/m^2}$, a peak at 20-200 $\mathrm{cd/m^2}$, and low sensitivity at luminances above 200 $\mathrm{cd/m^2}$. Indeed, the decrease at high photopic levels indicates a previously unreported failure of Weber's law; this is likely because other authors [19] only measured up to 1,000 $\mathrm{cd/m^2}$.

This luminance dependence interacted with spatial frequency, such that maximum sensitivity occurred between 20-200 $\mathrm{cd/m^2}$ for 1-2 cpd where observers could reliably detect a Gabor patch of 2-3% contrast. For red-green and yellow-violet modulations, contrast sensitivity rose as a function of luminance, reaching a maximum at around 200 $\mathrm{cd/m^2}$. A decrease in peak sensitivity was only observed at the lowest frequency.

Spatiochromatic Model

Achromatic CSF

We modeled the achromatic CSF as a log-parabola [1, 15, 20, 8]

$$\log_{10} S(f; S_{\max}, f_{\max}, b) \tag{1a}$$

$$= \log_{10} S_{\max} - \left(\frac{\log_{10} f - \log_{10} f_{\max}}{0.5 \cdot 2^b} \right)^2 \tag{1b}$$

where $S_{\max}$ was the peak sensitivity, expressed as the inverse of cone contrast, and $f_{\max}$ was the peak frequency in cpd. b was the bandwidth in dB, defined as the full-width at half-maximum. $S_{\max}$ and $f_{\max}$ were themselves modeled as functions of luminance:

$$\log_{10} S_{\max}(l) = 1.705 \exp\left[-\left(\frac{\log_{10} l - 1.867}{4.444} \right)^2 \right] \tag{2a}$$

$$f_{\max}(l) = 1.663 \exp\left[-\left(\frac{\log_{10} l - 3.045}{4.008} \right)^2 \right] \tag{2b}$$

We set $b = 1.036$, the median across individuals fits to each luminance level. The fits are shown in Fig. 5.

Chromatic CSFs

We modeled the chromatic CSF as a truncated log-parabola to describe the low-pass behaviour of chromatic contrast sensitivity measurements (Fig. 3):

$$S'(f; S_{\max}, f_{\max}, b) = \begin{cases} S_{\max} & \text{if } f < f_{\max} \\ S(f) & \text{otherwise} \end{cases} \tag{3a}$$

where $S(f)$ was the log-parabola (Eq. 1). For the red-green CSF,

$$\log_{10} S_{\max}(l) = 2.715 \exp\left[-\left(\frac{\log_{10} l - 2.663}{4.757} \right)^2 \right] \tag{4a}$$

$$f_{\max}(l) = 0.06069 \log_{10} l + 0.3394 \tag{4b}$$

and $b = 1.085$. For the yellow-violet CSF,

$$\log_{10} S_{\max}(l) = 1.843 \exp\left[-\left(\frac{\log_{10} l - 2.696}{3.688} \right)^2 \right] \tag{5}$$

$f_{\max} = 0.4095$ and $b = 1.097$.

The fits were good at low spatial frequencies, but at 4 and 6 cpd, the measured sensitivities were higher than those predicted by Eqs. 3, 4 and 5 (Fig. 5). As a purely chromatic mechanism

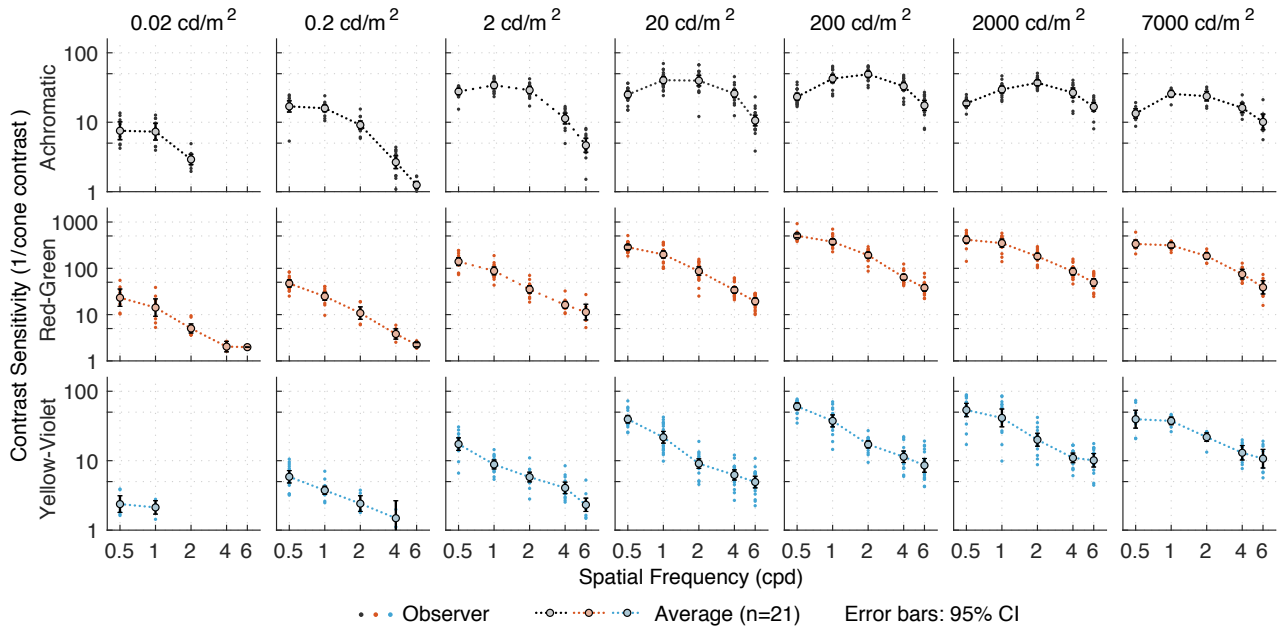

Figure 3: Contrast sensitivity measurements as a function of frequency.

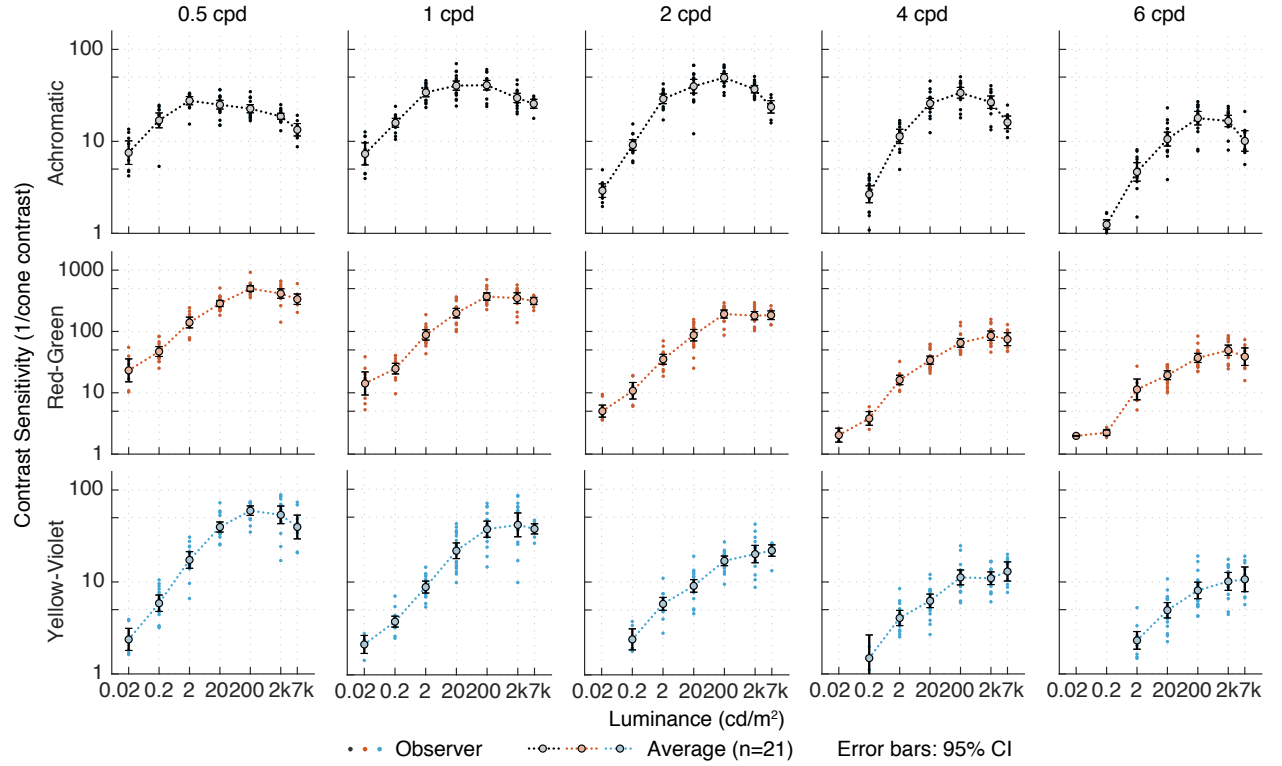

Figure 4: Contrast sensitivity measurements as a function of luminance.

is unlikely to detect contrast at spatial frequencies greater than 2 cpd [11], contrast sensitivity at 4 and 6 cpd likely indicated intrusion by the achromatic mechanism. This is likely because the stimuli were designed to be isoluminant for the average observer, not for each observer. See [23] for a model extension that accounts for luminance intrusion.

Spatial Summation

Spatial patterns are easier to detect when they are larger on the retina. To account for this effect, we adapted the model of spatial summation from [16], which describes contrast sensitivity as a saturating function of area:

$$S_A(f,a;S_{\max},f_{\max},b,a_0,f_0) = S(f;S_{\max},f_{\max},b)\sqrt{\frac{af^2}{a_0+af_0+af^2}}, \quad (6)$$

where $S(f;S_{\max},f_{\max},b)$ was our CSF (Eq. 1, 3), f was the spatial frequency in cpd and a was the stimulus area in deg^2. As our stimuli did not have sharply defined boundaries, we approximated a with $\pi\sigma^2$, where σ was the standard deviation of the Gaussian envelope. a_0 and f_0 were free parameters that controlled the rate of saturation.

To validate the model, we measured contrast sensitivities

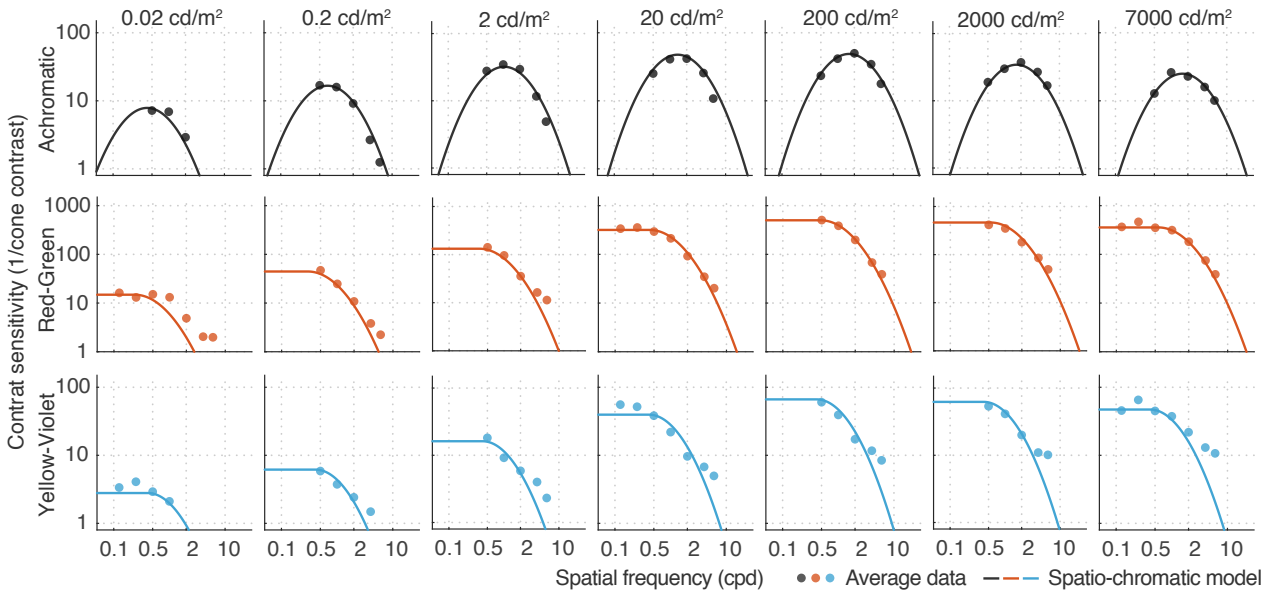

Figure 5: Contrast sensitivity predictions as a function of background luminance. Red-green and yellow-violet CSFs include additional data at $f = 0.125, 0.25°$ for $l = 0.02, 20, 7000\,\mathrm{cd/m^2}$ from [23].

at $20\,\mathrm{cd/m^2}$ for Gabor patches with envelopes $\sigma = 0.25f^{-1}$, $0.5f^{-1}$, $1f^{-1}$, and $2f^{-1}$. We set $a_0 = 114$ and $f_0 = 0.65$ for the achromatic CSF, and $a_0 = 40$ and $f_0 = 0.65$ for both chromatic CSFs [16]. The model fits were good for achromatic contrast sensitivities, as well as for chromatic sensitivities at $f \leq 2$ cpd, though predictions were less accurate for chromatic channels at 4 and 6 cpd due to luminance intrusion (Fig. 6).

To extend the spatial summation model to other luminances, we assumed little interaction between the effects of luminance and stimulus size [10]. We modeled the effect of luminance as the ratio between the sensitivity at the desired luminance l (Eq. 1) and the sensitivity at $20\,\mathrm{cd/m^2}$ (for which we fitted the spatial summation model, Fig. 6):

$$S_{AL}(f,l,a) = \gamma S_A(f,a) = \frac{S_L(f,l)}{S_L(f,20)} \cdot S_A(f,a)\,. \qquad (7)$$

S_A was the area-dependent CSF (Eq. 6), and γ was the gain parameter. The parameters of $S_L(f,20)$ were $S_{\max} = 447.5$, $f_{\max} = 1.105$, $b = 0.6764$ for the achromatic CSF, $S_{\max} = 2780$, $f_{\max} = 0.1321$, $b = 1.832$ for the red-green CSF, and $S_{\max} = 555.7$, $f_{\max} = 0.04399$, $b = 2.397$ for the yellow-violet CSF.

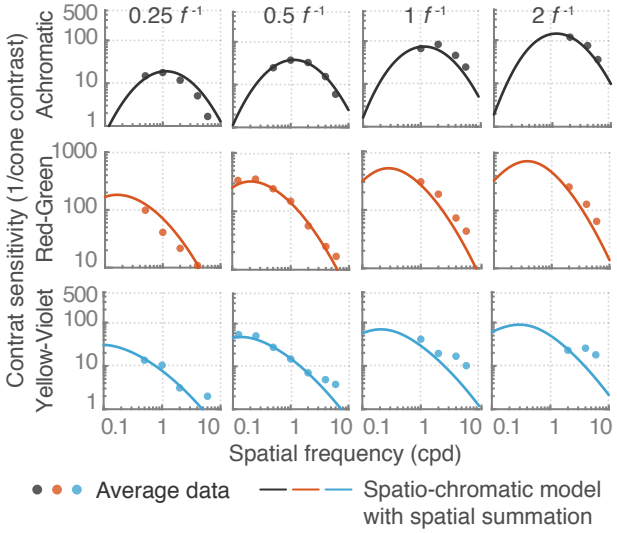

Figure 6: Contrast sensitivity predictions at fixed stimulus sizes.

Preliminary results show that the spatio-chromatic model with spatial summation is promising. With only one additional gain parameter, Equation 7 made reasonable predictions of data from [22] (Fig. 7). As [22] used different stimulus and experiment design from our experiment, it is encouraging that the model makes reasonably good predictions. See [23] for details of predicting other datasets.

Conclusions

We measured contrast sensitivities over a wide range of frequencies, colors, and luminances. For achromatic contrast, we replicated known findings, such as the Weber law at photopic levels. However, we also discovered a failure of Weber law: contrast sensitivity decreased at luminances above $200\,\mathrm{cd/m^2}$. Chromatic contrast, on the other hand, increased monotocally with background luminance, asymptoting at $200\,\mathrm{cd/m^2}$. We do not have a mechanistic explanation for this difference at the moment. Regardless, our dataset provides an important resource for future work on HDR displays.

We developed a model to account for our data, and proposed an extension to account for spatial summation. While the there is still work to be done, preliminary results are promising.

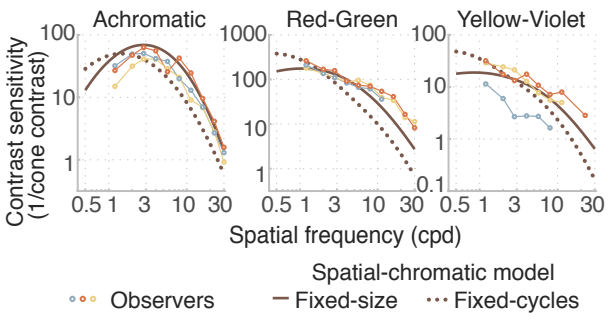

Figure 7: Proposed spatio-chromatic model prediction of published data [22]. [22] used Gabor patches with the same σ for all frequencies ('fixed-size'), such that the stimuli subtended the same region, but showed different number of cycles.

Acknowledgments

This project has received funding from the European Research Council (ERC) under the European Union's Horizon 2020 research and innovation programme (grant agreement N° 725253–EyeCode) and from EPSRC research grant EP/P007902/1, EP/P007503, EP/P007910, EP/P007600.

References

[1] Albert J Ahumada, Jr and Heidi A Peterson. Luminance-model-based DCT quantization for color image compression. In *Human vision, visual processing, and digital display III*, volume 1666, pages 365–374. International Society for Optics and Photonics, 1992.

[2] Roy S. Berns. Methods for characterizing CRT displays. *Displays*, 16(4):173–182, may 1996.

[3] F. W. Campbell, J. J. Kulikowski, and J. Levinson. The effect of orientation on the visual resolution of gratings. *The Journal of Physiology*, 187(2):427–436, 1966.

[4] Fergus W Campbell and JG Robson. Application of fourier analysis to the visibility of gratings. *The Journal of physiology*, 197(3):551, 1968.

[5] CIE170-1:2006. Fundamental chromacity diagram with psychological axes - part 1. Technical report, Central Bureau of the Commission Internationale de l'Éclairage, 2006.

[6] A. M. Derrington, J. Krauskopf, and P. Lennie. Chromatic mechanisms in lateral geniculate nucleus of macaque. *The Journal of Physiology*, 357(1):241–265, 1984.

[7] Clarence Henry Graham and Rodolfo Margaria. Area and the intensity-time relation in the peripheral retina. *American Journal of Physiology-Legacy Content*, 113(2):299–305, 1935.

[8] Yeon Jin Kim, Alexandre Reynaud, Robert F Hess, and Kathy T Mullen. A normative data set for the clinical assessment of achromatic and chromatic contrast sensitivity using a qcsf approach. *Investigative ophthalmology & visual science*, 58(9):3628–3636, 2017.

[9] Mario Kleiner, David Brainard, and Denis Pelli. What's new in psychtoolbox-3? 2007.

[10] Rafal Mantiuk, Kil Joong Kim, Allan G. Rempel, and Wolfgang Heidrich. HDR-VDP-2: A calibrated visual metric for visibility and quality predictions in all luminance conditions. *ACM Transactions on Graphics*, 30(4):40:1—-40:14, jul 2011.

[11] KT Mullen. The contrast sensitivity of human colour vision to red-green and blue-yellow chromatic gratings. *The Journal of physiology*, 359:381400, February 1985.

[12] Juvi Mustonen, Jyrki Rovamo, and Risto Näsänen. The effects of grating area and spatial frequency on contrast sensitivity as a function of light level. *Vision Research*, 33(15):2065 – 2072, 1993.

[13] C. Noorlander, M. G. Heuts, and J. J. Koenderink. Influence of the target size on the detection threshold for luminance and chromaticity contrast. *Journal of the Optical Society of America*, 1980.

[14] J. Gordon Robson and N. V. S. Graham. Probability summation and regional variation in contrast sensitivity across the visual field. *Vision Research*, 21:409–418, 1981.

[15] Ann Marie Rohaly and Cynthia Owsley. Modeling the contrast-sensitivity functions of older adults. *JOSA A*, 10(7):1591–1599, 1993.

[16] Jyrki Rovamo, Olavi Luntinen, and Risto Näsänen. Modelling the dependence of contrast sensitivity on grating area and spatial frequency. *Vision Research*, 33(18):2773–2788, 1993.

[17] Helge Seetzen, Wolfgang Heidrich, Wolfgang Stuerzlinger, Greg Ward, Lorne Whitehead, Matthew Trentacoste, Abhijeet Ghosh, and Andrejs Vorozcovs. High dynamic range display systems. *ACM Transactions on Graphics*, 23(3):760, aug 2004.

[18] Simon Shlaer. The relation between visual acuity and illumination. *The Journal of general physiology*, 21(2):165–188, 1937.

[19] Floris L. Van Nes and Maarten A. Bouman. Spatial modulation transfer in the human eye. *J. Opt. Soc. Am.*, 57(3):401–406, Mar 1967.

[20] Andrew B. Watson and Albert J. Ahumada. A standard model for foveal detection of spatial contrast. *Journal of Vision*, 5(9):717–740, 2005.

[21] Andrew B Watson and Denis G Pelli. Quest: A bayesian adaptive psychometric method. *Perception & psychophysics*, 33(2):113–120, 1983.

[22] S.M. Wuerger, A.B. Watson, and A. Ahumada. Towards a spatio-chromatic standard observer for detection. In *Proceedings of SPIE - The International Society for Optical Engineering*, volume 4662, 2002.

[23] Sophie Wuerger, Maliha Ashraf, Minjung Kim, Jasna Martinovic, María Pérez-Ortiz, and Rafał K. Mantiuk. Spatio-chromatic contrast sensitivity under mesopic and photopic light levels. *Journal of Vision*, in print, 2019.

Author Biography

Minjung Kim is a postdoctoral research associate at the Department of Computer Science and Technology, University of Cambridge. Her PhD is from New York University and York University, Canada. Her research interests include the perception of color, light, and shape, and the computational modeling of visual perception. `https://www.minjung.ca`

Maliha Ashraf is a PhD student at the Cognitive and Clinical Neuroscience Group and the Department of Engineering at the University of Liverpool. She has a Erasmus Mundus Joint Master Degree in Color in Science and Industry. Her research interests are color vision and display technologies. `https://www.linkedin.com/in/malihaashraf/`

Maria Pérez-Ortiz is a postdoctoral research fellow at University College London. Previously she was a postdoctoral research associate at the University of Cambridge. Her research interests include machine learning and its applications. `http://mariaperezortiz.com/`

Jasna Martinovic is a Senior Lecturer at the University of Aberdeen. Her PhD is from the University of Leipzig. She is interested in how visual signals enter mid and higher-level stages of perception, and in categorical effects of color perception and appearance. `https://sites.google.com/site/drjasnamartinovic/home`

Sophie Wuerger is a Professor at the University of Liverpool. She received her PhD from New York University. She is interested in understanding how retinal signals map into higher-order appearance mechanisms. `https://pcwww.liv.ac.uk/~sophiew/`

Rafał K. Mantiuk is a Reader at the University of Cambridge. His PhD is from the Max-Planck-Institut für Informatik. He contributed to early work on high dynamic range imaging. He works on display, imaging and rendering methods that benefit from the limitations of visual perception. `https://www.cl.cam.ac.uk/~rkm38/`